Metabolic Brain Disease
https://doi.org/10.1007/s11011-022-01029-x

ORIGINAL ARTICLE

Long term high fat diet induces metabolic disorders and aggravates behavioral disorders and cognitive deficits in MAPT P301L transgenic mice

Jing Xiong[1,2] · Isaac Deng[1] · Sally Kelliny[1,3] · Liying Lin[1] · Larisa Bobrovskaya[1] · Xin-Fu Zhou[1]

Received: 26 April 2021 / Accepted: 7 June 2022

Abstract

Most Alzheimer disease (AD) patients present as sporadic late onset AD, with metabolic factors playing an important role in the occurrence and development of AD. Given the link between peripheral insulin resistance and tau pathology in streptozotocin-injected and db/db mouse models of diabetes, we fed high fat diet (HFD) to pR5 mice expressing P301L mutant human tau, with the aim of developing a new model with characteristics of obesity, T2DM and AD to mimic AD patients exacerbated by obesity and T2DM, an increasing trend in modern society. In our study, pR5 and C57BL/6 (WT) mice were randomly allocated to a standard diet (STD) or HFD for 30 weeks starting at 8 weeks of age. Food intake was measured weekly, body weight and fasting glucose levels were measured fortnightly, and a comprehensive behavioral test battery was performed to assess anxiety, depression and cognitive dysfunction. Glucose and insulin tolerance tests were performed after 30 weeks of HFD. We also investigated the effect of long term HFD on tau pathology in the brains of WT and P301L mice by performing western blotting of whole brain homogenates for total tau, phosphorylated tau at Ser396 and Thr231. Our results show that pR5 mice fed with HFD are more vulnerable to diet induced obesity compared to WT, especially with increasing age. In addition, pR5 mice on HFD developed glucose intolerance and insulin resistance. It was identified that long term HFD significantly aggravates depression like behavior and impairs cognitive function in pR5 mice, and also induces anxiety like behavior in both pR5 and WT mice. Long term HFD was also shown to aggravate tau hyperphosphorylation in pR5 transgenic mice, and increase total and hyperphosphorylated tau in WT mice. These results indicate that diet induced obesity of pR5 transgenic mice expressing P301L mutant human tau generates T2DM, and aggravates tau phosphorylation, and is therefore a model useful for investigations that seek to understand the relationships between AD, T2DM and obesity, and the underlying biochemical changes and mechanisms associated with metabolic disorders and AD tauopathy.

Keywords High fat diet · Obesity · T2DM · Alzheimer disease · Tauopathy

Introduction

With the aging of the world's population, adults living with dementia are predicted to reach around 150 million by 2050, with Alzheimer disease (AD) accounting for 60% ~ 80% of dementia patients (Kullmann et al. 2016). AD is characterized by a progressive decline in memory and other cognitive functions associated with neuronal loss, resulting in dementia. Most AD patients present as sporadic and late onset. Metabolic factors play an important role in the occurrence and development of AD (Gong et al. 2016).

It is well known that chronic obesity and type 2 diabetes mellitus (T2DM) are often associated with AD, along with many other comorbidities, including cardiovascular disease, and renal dysfunction. Moreover, obesity and T2DM

Highlights
- HFD induced obesity of pR5 transgenic mice expressing P301L mutant human tau generates T2DM.
- HFD induces glucose intolerance and insulin resistance in pR5 mice.
- pR5 mice are more vulnerable to HFD induced obesity compared to WT especially with increasing age.
- pR5 mice are more vulnerable to HFD induced glucose intolerance impairment compared to WT especially with increasing age.
- Long term HFD significantly aggravates depression like behavior and cognitive deficit in pR5 mice.
- Long term HFD aggravates tau hyperphosphorylation in pR5 transgenic mice.

Extended author information available on the last page of the article

Published online: 15 June 2022

are increasingly linked to impaired central nervous system (CNS) function, by exacerbating psychiatric and cognitive disorders, including mood disorders, cognitive decline and dementias (Anderson et al. 2001; Platt et al. 2016). Due to improved therapeutics, individuals with T2DM are living longer into the ages where they are at a greater risk of developing neurodegenerative diseases such as Alzheimer disease (AD), mild cognitive impairment, and vascular dementia, compared to healthy counterparts of similar age (Platt et al. 2016). Furthermore, unhealthy lifestyle habits, and excessive energy intake in general, are major contributing factors to the increased prevalence of obesity and T2DM, further augmenting the burden of cognitive impairment throughout the world (Hryhorczuk et al. 2013; Kanoski and Davidson 2011).There is also a bidirectional association between T2DM and AD. The major pathological features of AD are amyloid plaques, which are made up of aggregates of β-amyloid protein, and neurofibrillary tangles (NFT's), consisting of hyperphosphorylated tau protein (Kandimalla et al. 2017). Tau hyperphosphorylation is also observed in other neurodegenerative diseases, such as frontotemporal dementia (FTD), and Parkinson's disease (Platt et al. 2016). Increased tau phosphorylation has been reported in diabetic animal brains including type 1 (streptozotocin-injected) and type 2 (db/db) mouse models of diabetes (Clodfelder-Miller et al. 2006; Freude et al. 2005; Jolivalt et al. 2008; Planel et al. 2007). Peripherally injected Streptozotocin (STZ), a chemical compound toxic to pancreatic β-cells, induces type 1 diabetes, generating tau hyperphosphorylation in the mouse brain (Papon et al. 2013; Planel et al. 2007). This establishes a link between peripheral insulin resistance and tau pathology, and the db/db mouse model of leptin deficiency, widely used as a model of T2DM, also shows increased tau phosphorylation in the cortex and hippocampus compared to controls.

Insulin resistance is a metabolic compromise generally associated with obesity and favoring the occurrence of T2DM. It has been shown in postmortem brains of patients and experimental models of obesity, that there are defects in brain insulin signaling (Mullins et al. 2017). Defective insulin signaling and altered glucose metabolism have also been found in AD, with defective insulin signaling being identified in postmortem brains of AD patients (Liu et al. 2011; Talbot et al. 2012).

Tau hyperphosphorylation could relate to defective peripheral insulin signaling. The N-terminal of tau protein binds to the SH3 domain of Src family tyrosine kinase, including phosphatidylinositol 3-kinase (PI3K), a key protein in the insulin signaling pathway (Reynolds et al. 2008). PI3K plays an important role in regulating insulin signaling (Goncalves et al. 2019). Knocking out the tau gene led to impaired sensitivity of the hippocampus to insulin (Marciniak et al. 2017). Recently, it has been found that the phosphorylation of tau protein is related to brain and peripheral insulin resistance, and β cell dysfunction. Tau protein is highly expressed in β cells of the pancreas, and regulates peripheral glucose metabolism. Mice with knocked out tau gene, show increased body weight, and impairment of insulin and glucose tolerance at a very young age (Wijesekara et al. 2018).

According to published studies, high fat diet induces obesity and glucose metabolism disorder in C57BL/6 mice, which is a common T2DM and insulin resistance model (Winzell and Ahren 2004). This model is similar to the process of human obesity and metabolism disorder caused by high fat food in modern society. Given the link between peripheral insulin resistance and tau pathology in streptozotocin-injected and db/db mouse models of diabetes, it is important to know the impacts of HFD on glucose metabolism and the behaviors of tau transgenic mice, which are currently unreported. The MAPT P301L (pR5 strain) mouse line overexpresses the P301L mutation, producing the mutant human tau that constitutes the brain tangles found in Alzheimer disease (Gotz et al. 2001). In these mice, pronounced tau hyperphosphorylation is initially detected in the amygdala and subsequently in the CA1 region of the hippocampus at about 6 months of age, resulting in behavioral impairments in amygdala and hippocampus dependent functions (Pennanen et al. 2006). Observational studies of individuals in late midlife with diabetes show 24% faster cognitive decline than those without diabetes. Additionally, midlife obesity and T2DM have both been shown to be related to dementia (Bandosz et al. 2020).

Based on this evidence, we administered long term HFD to pR5 transgenic mice when the mice were 8 weeks old, to 38 weeks old, and investigated the variations in glucose levels, behavior impairments, and learning/memory function. In the present study, long term HFD induces metabolism disorders in WT and pR5 mice, and aggravates behavioral impairments, and cognitive deficits in pR5 mice.

Materials and methods

Ethics statement

These experiments were conducted in accordance with the NIH Guide for the Care and Use of Laboratory Animals. All protocols were approved by the Animal Ethics Committee at the University of South Australia, Australia (U41-16).

Animals and housing

Female pR5 mice (C57BL/6 background) expressing P301L mutant human tau (n = 16) were generated by overexpression of human four-repeat tau mutated at sites G272V and

Table 1 Study cohorts and diet treatments

Study cohorts and diet treatments				
Diet weeks	pR5 mice n = 16		WT mice n = 16	
Weeks 0–8	STD		STD	
Weeks 9–38	STD n = 8	HFD n = 8	STD n = 8	HFD n = 7*

* One death in wildtype on high fat diet, cause unknown

P301S under the control of Thy1.2 promoter (Gotz et al. 2001; Ke et al. 2009). C57BL/6 mice (WT) were used as controls (n = 16). Sample size determination based on our previous published works using study cohorts of low genetic variability, we made the following assumptions: For biochemical parameters, SD values will be 20% of means, and for behavioral tests, SD values will be 30% of means. Effect size for biochemical measures, will be 20–30% of controls, and for cognitive testing, the effect size will be 20% with greater variation, The power calculation was carried out using the parameters for behavioral testing, as these have the higher variability. We used power level (1-beta) of 90% and statistical significance (alpha) of 0.05.

A total of 31 female mice were housed under standard pathogen free conditions (room temperature 22 °C and humidity of 55%) with food and water ad libitum and regular 12:12 light–dark cycle. Table 1 shows the study groups and duration of diet treatments. All mice were fed STD for the first 8 weeks. At 8 weeks of age, C57BL/6 (WT) mice and pR5 transgenic mice were paired by the same sex, same nest and similar weight, and then were randomly placed into STD or HFD groups, (i) wildtype with standard diet (WT STD, n = 8); (ii) wildtype with high fat diet (WT HFD, n = 7, there was one death in wildtype with high fat diet and the cause was unable to be determined); (iii) pR5 transgenic mice with standard diet (pR5 STD, n = 8) and (iv) pR5 transgenic mice with high fat diet (pR5 HFD, n = 8). Analysis of experimental results was blinded.

Nutritional parameters of the STD and HFD

Standard diet (STD) and high fat diet (HFD) formulation in the present study are from Specialty Feeds, Western Australia. All nutritional parameters of STD meet or exceed the NRC guidelines for rats and mice. High fat diet (SF04-001 formulation from Specialty Feeds, Western Australia), a semi-pure high fat diet formulation for laboratory rats and mice is based on Research Diets D12451. Some modifications have been made to the original formulation to suit locally available raw materials for research studies on metabolic disorders.

The nutritional parameters of the STD were protein 20.00%, total fat 4.80%, crude fiber 4.80%, acid detergent fiber 7.60%, neutral detergent fiber 16.40%, total carbohydrate 59.40%, digestible energy 14.0 MJ / Kg, % total calculated energy from protein 23.00%, % total calculated energy from lipids 12.00%. The nutritional parameters of the HFD were 22.60% protein, total fat 23.50%, crude fiber 5.40%, acid detergent fiber 5.40%, digestible energy 19 MJ / Kg, % total calculated digestible energy from protein 21.00%, % total calculated digestible energy from lipids 43.00%.

Food energy intake and body weight for STD and HFD

WT and pR5 mice were given STD until 8 weeks old. Half of the mice from each group (WT and pR5 mice) were given HFD starting at 8 weeks of age and the treatment continued for 30 weeks when the mice were 38 weeks of age. The other half from each group was used as controls and continued to receive the STD for the same period of time. The mice were housed in groups and the food intake was measured weekly. The food for each of the cages was changed weekly.

Food intake was obtained by subtracting from the initial weight of the food, the final weight including any food pellets that had spilled into the cage (Ellacott et al. 2010). The weekly caloric intake was then analyzed separately for each of the 4 groups. The body weight of all the animals was measured every two weeks starting from 8 weeks of age to 38 weeks of age (duration 30 weeks).

Fasting blood glucose levels, glucose and insulin tolerance test

The fasting glucose levels were measured every 2 weeks after the initiation of the HFD. Firstly, the mice were fasted overnight for approximately 16 h in order to closely mimic the human glucose tolerance test. Blood samples were then taken from the tail vein and the blood glucose levels were measured using a glucometer (Breeze2, Bayer HealthCare, LLC; Tarrytown, NY). After 30 weeks of high fat diet, we performed glucose tolerance tests (GTT) to assess insulin secretion, insulin action and effectiveness, the ability of insulin to effectively reduce glucose levels (Andrikopoulos et al. 2008).

Prior to the GTT, mice were fasted for approximately 16 h. Baseline glucose levels were then measured before an intraperitoneal (IP) injection of glucose (1 g/kg body weight). Repeated blood glucose measurements were taken at 15, 30, 60, 90 and 120 min after the glucose injection. Insulin tolerance tests (ITT) were performed to test whether or not insulin sensitivity was impaired by HFD. For ITT, mice were fasted for 5 h prior to the test. Baseline glucose levels were then measured, and body weights of the mice were taken before an intraperitoneal injection of insulin

(0.75 IU/kg). Blood glucose levels were then measured at 15, 30, 60, 90 and 120 min after insulin injection.

Behavioral tests

Anxiety-like behavior and depression-like behavior tests

The amygdala and hippocampus are among the initial structures that are affected by tau pathology in AD, resulting in behavioral impairments such as anxiety and memory deficits (Cavedo et al. 2014; Poulin et al. 2011). Thus, we investigated whether pR5 mice on HFD present with specific behavioral changes compared with the STD groups and WT HFD mice.

Elevated plus maze tests were performed to assess amygdala related anxiety levels. The elevated plus maze apparatus has two open arms and two enclosed arms elevated approximately 1 m above the ground. We measured distance in the open arms, time spent in the open arms and entries into the open arms using the ANY-maze tracking system (Stoelting co., Wood Dale, IL, USA) for a duration of 5 min (Belovicova et al. 2017; Walf and Frye 2007). Depression like behavior was assessed in the forced swim and tail suspension tests which measure the immobility time of the animals as a representation of behavioral despair. In the forced swim test, the mice were placed in a transparent cylinder containing water.

Immobility time was recorded during the last 4 min of the 6 min test session using ANY-maze software and the percentage of immobility time was calculated. In the tail suspension test, the mice were suspended by the tail with an adhesive tape, approximately 35 cm above the ground. The mice were continuously monitored for 6 min using ANY-maze software and the immobility time was recorded and the percentage of immobility time was calculated.

Recognition memory

Recognition memory and tendency of mice to explore new objects was evaluated by the novel object recognition test (Kelliny et al. 2021). Prior to testing, each animal was habituated to the testing arena for 5 min. Following habituation, each animal was allowed to explore two identical objects placed symmetrically from the arena center for 5 min (sample phase). Two hours later, one of the familiar objects was replaced with a novel object and again each animal was allowed to explore the two objects (the sample and the novel objects) for 5 min (test phase). We measured the novel object exploration distance, time, and entries. Ratios were calculated by dividing the total distance, time and entries to explore both objects and multiplied by 100.

Spatial reference memory

We used the Morris's water maze test to measure spatial reference memory (Nunez 2008; Vorhees and Williams 2006). The water maze apparatus consists of a circular polypropylene pool (120 cm diameter × 45 cm height), with four different patterns of cues surrounding the pool to assist the mice with navigation. The pool was filled with water, maintained at 23 ± 1 °C, and a non-toxic white paint was added to make the water opaque. In the pre training, a 2 min free-swim session was conducted to acclimate the mice to the environment. In addition, the mice undertook visible platform training, whereby the platform was situated 0.5 cm above the water, and they were allowed to swim for 60 s for three trials. If the mice could not locate the platform in the given time, they were guided to the location. Once the pre training was completed, the platform was submerged 0.5 cm below the water, and the mice were allowed to find the hidden platform (3 trials, 60 s per a trial) and this assessment was carried out daily for 4 days. After the hidden platform session, the mice were subjected to the probe test whereby the platform is removed, and the mice were given 60 s to explore the pool.

Immunohistochemistry (IHC)

Serial 5-µm-thick sections of paraffin-embedded tissues were cut using a microtome, and then mounted on poly-L-lysine coated slides. Single-label IHC was carried out using the avidin–biotin peroxidase method and diaminobenzidine as the chromogen. Sections were deparaffinized in xylene, then brought to water through a graded series of ethanol. Sections were incubated in 3% H_2O_2(Cat. No. 88,597, Millipore) for 10 min to block endogenous peroxidase. Sections were subjected to antigen heat retrieval in citrate buffer (pH 6.0) using a pressure cooker and then washed with PBS (pH 7.4, Cat. No.P3813, Sigma-Aldrich). Sections were blocked for 1 h with 10% normal horse serum before applying the primary antibodies (see Table 2), and then incubated at 4℃ overnight. After incubation with the primary antibodies, sections were washed in PBS 3 times and then incubated with the appropriate biotinylated secondary antibody (1:200 goat anti-rabbit, Cat. No.sc-2040, or 1:200 goat anti mouse immunoglobulin, Cat.No. sc-2039; both from Santa Cruz) at room temperature for 1 h. All sections were incubated with avidin–biotin peroxidase complex (Vectastain ABC kit, Cat.No.PK-4000 Vector Labs) at room temperature for 30 min, then developed in a solution of diaminobenzidine (Cat.No. D800, Sigma-Aldrich) and counterstained with hematoxylin. Sections were

Table 2 Primary antibodies used in this study

Antibody	Type/Host	Specificity	Source	Cat. No.	Dilution for IHC	Dilution for WB
Tau 5	Monoclonal/ mouse	Mouse Tau	Thermo Fisher	AHB0042	1:100	1:1000
p(Ser396) -tau	Monoclonal/ Rabbit	pTau at Ser 396	Abcam	ab156623	1:600	1:5000
p(Thr231)-tau	Monoclonal/ Rabbit	pTau at Thr 231	Abcam	ab151559	1:400	1:1000
GAPDH	Polyclonal/ Rabbit	GAPDH	Osenses	OSG00032W	-	1:5000

Specificity of antibodies is assumed based on manufacturer guarantee. Abcam: - validation by Knock-out (KO), Thermo Fisher:- validation by relative expression

dehydrated through a graded series of alcohol washes, cleared in xylene, then coverslipped. Slides were scanned with a NanoZoomer S60 Automated Digital slide scanner (Hamamatsu Photonics). Image analysis was performed with Image J software (NIH, Bethesda, MD, USA).

Western blotting analysis

Animals were humanely killed by inhalation of CO_2, then transcardially perfused with ice cold saline. Brain tissues were harvested from each mouse and homogenized in liquid nitrogen, and then sonicated in RIPA buffer (50mM Tris-HCl (Cat.No.10,812,846,001, Roche), 150mM NaCl (Cat.No.S9888,Sigma-Aldrich, 2mM EDTA (Cat.No.E9884, Sigma-Aldrich), 0.1% SDS (Cat.No.L3771,Sigma-Aldrich), 1% Sodium deoxycholate (Cat.No.D6750, Sigma-Aldrich) and 1% Nonidet-40) (pH 7.4, Cat.No.ab142227,Abcam) at 4 °C containing protease and phosphatase cocktail inhibitors. Homogenates were centrifuged at 15,000 rpm for 30 min and the supernatants collected. Total proteins were measured using BCA total protein assay kit (Cat. No. ab102536,Abcam). Samples of equal protein concentrations were separated on 10–12% SDS-PAGE and electro-transferred onto 0.2 µm nitrocellulose membranes. The membranes were then blocked with 5% milk in Tris-HCl buffer with 0.5% Tween 20 for 2 h at room temperature and incubated overnight at 4 °C with primary antibodies in TBST containing 5% nonfat milk (see Table 2 for the primary antibodies used in the present study). After several washes in TBST, the membranes were incubated with the appropriate horseradish peroxidase–conjugated secondary antibodies (goat anti-rabbit (Cat.No. sc-2030) or anti-mouse (Cat.No.sc-2031) in TBST + 5% nonfat milk, 1:1000; all Santa Cruz) for 2 h at room temperature. After washing with TBST, immunoreactive bands were detected using an enhanced chemiluminescence kit (Cat.No.CW0048, CoWin Biotechnology). Densitometric analyses were performed using Image Studio Lite software (Li-COR Bioscience). Protein density was determined in relative units in reference to GAPDH.

Statistics

All data sets were checked for normality using Shapiro–Wilk's test, with appropriate statistical tests selected, based on the results. Homogeneity of variance was assessed using the Levene test. The results of tests for normality and variance homogeneity for each experiment are in supplement 1. Data sets distributed normally are presented as means ± Standard Deviation (S.D.), and statistical comparisons made by using one-way analysis of variance, (ANOVA) followed by a post hoc LSD test for multiple comparisons. Data sets not normally distributed are presented as median and interquartile ranges, and a non-parametric Kruskal–Wallis test used, followed by Dunn's test for post hoc analysis. All statistical analyses were performed with SPSS software (version 13.0) in a blinded manner.

Results

HFD and genotype modulate food intake and body weight

Standard diet (STD) and high fat diet (HFD) were fed to the respective groups. Obesity is established by higher energy intake due to HFD treatment. As Fig. 1a shows, both WT and pR5 mice on HFD had higher energy intake compared to their corresponding control groups on STD throughout the dietary period. The energy intake increased drastically in the first two weeks on HFD for both pR5 and WT, but progressively decreased after 4 weeks of HFD, with the difference between pR5 STD and WT STD groups being stable. Notably, compared to WT HFD mice, a larger caloric intake in pR5 HFD mice was observed after 4 weeks of HFD, and this continued until the end of the dietary period.

In body weight gain comparisons (Fig. 1b), both WT and pR5 mice on HFD increased significantly greater than mice on STD after 2 weeks of diet treatment, staying significantly different through the remaining weeks. There was a higher body weight gain in pR5 HFD mice after 4

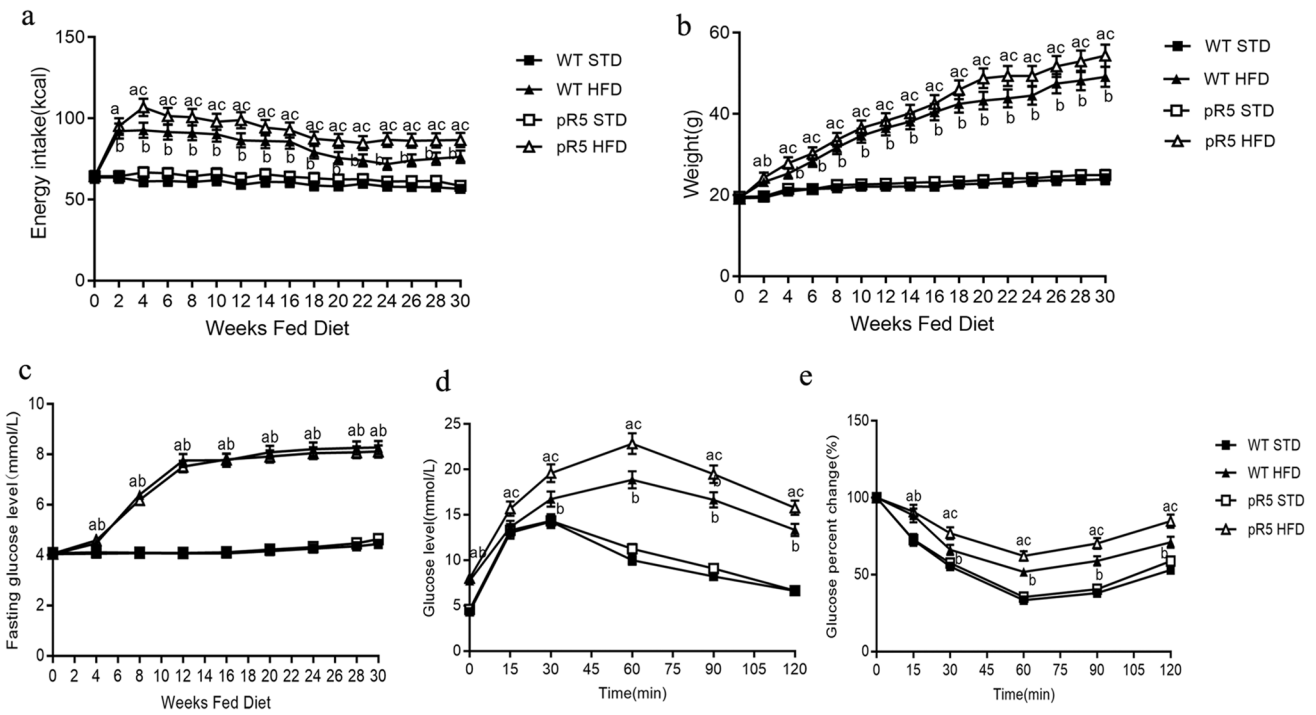

Fig. 1 HFD and genotype modulate food intake, body weight and glucose homeostasis. **a**. Energy intake in kcal. **b**. Body weight gain. The values are presented as median and interquartile ranges, and between group comparisons were analyzed using the Kruskal–Wallis test followed by Dunn's test for post hoc analysis. **c** Fasting blood glucose levels. The values are presented as mean ± S.D., and between group comparisons were analyzed using the ANOVA post hoc test. **d**. Glucose tolerance test. The values are presented as median and interquartile ranges, and between group comparisons were analyzed using the Kruskal–Wallis test followed by Dunn's test for post hoc analysis. **e**. Insulin resistance test. The values are presented as median and interquartile ranges, and between group comparisons were analyzed using the Kruskal–Wallis test followed by Dunn's test for post hoc analysis. "a" indicates $p < 0.01$, pR5 HFD vs. pR5 STD; "b" indicates $p < 0.05$, WT HFD vs. WT STD; "c" indicates $p < 0.05$, pR5 HFD vs. WT HFD

weeks on HFD, continuing thereafter to be progressively higher in pR5 HFD mice when compared with WT HFD mice. Significant augmented growth was observed in pR5 HFD fed mice from 18 weeks (Fig. 1b). As Fig. 1 shows, energy intake was increased in HFD fed mice compared with STD mice throughout the study period. As caloric intake remained steady after 4 weeks in the HFD treatment groups, weight gain continued, indicating that metabolic efficiency was reduced in the HFD fed mice. Compared to WT HFD mice, larger caloric intake and higher weight gains were observed in pR5 HFD mice after 4 weeks HFD treatment. These findings indicate that pR5 mice are vulnerable to diet induced obesity especially at older age compared to WT mice.

HFD and genotype modulate glucose homeostasis in pR5 and WT mice

Fasting glucose, ITT and GTT assays were performed to check establishment and status of T2DM. Fasting glucose levels were significantly higher in WT and pR5 mice on HFD at 4 weeks compared to the corresponding WT and pR5 mice on the STD (Fig. 1c). The average fasting glucose levels at 4 weeks were 4.5 mmol/L for WT HFD mice, versus 4.06 mmol/L for WT STD mice, with 4.56 mmol/L for pR5 HFD mice, versus 4.11 mmol/L for pR5 STD mice. Fasting glucose levels increased sharply in the 12 weeks after high fat diet was given. Thereafter, fasting glucose levels were steadily higher until the end of the experimental period at 30 weeks (fasting glucose at week 30: 8.22 mmol/L versus 4.16 mmol/L for WT HFD and WT STD mice respectively, and 8.05 mmol/L versus 4.21 mmol/L for pR5 HFD and pR5 STD mice respectively). There was no significant difference in the fasting glucose levels between WT and pR5 mice on the STD.

Impaired insulin function in T2DM is characterized by delayed or decreased insulin secretion, resulting in deterioration of glucose elimination. In our study, we performed the GTT after 30 weeks of HFD to assess glucose homeostasis (Fig. 1d). For GTT, a glucose load of 1 g/kg was administered through intraperitoneal (IP) injection and blood glucose levels were measured at 0, 15, 30, 60, 90 and 120 min after glucose treatment. Glucose tolerance impairment was observed in the WT HFD and pR5 HFD groups, showing

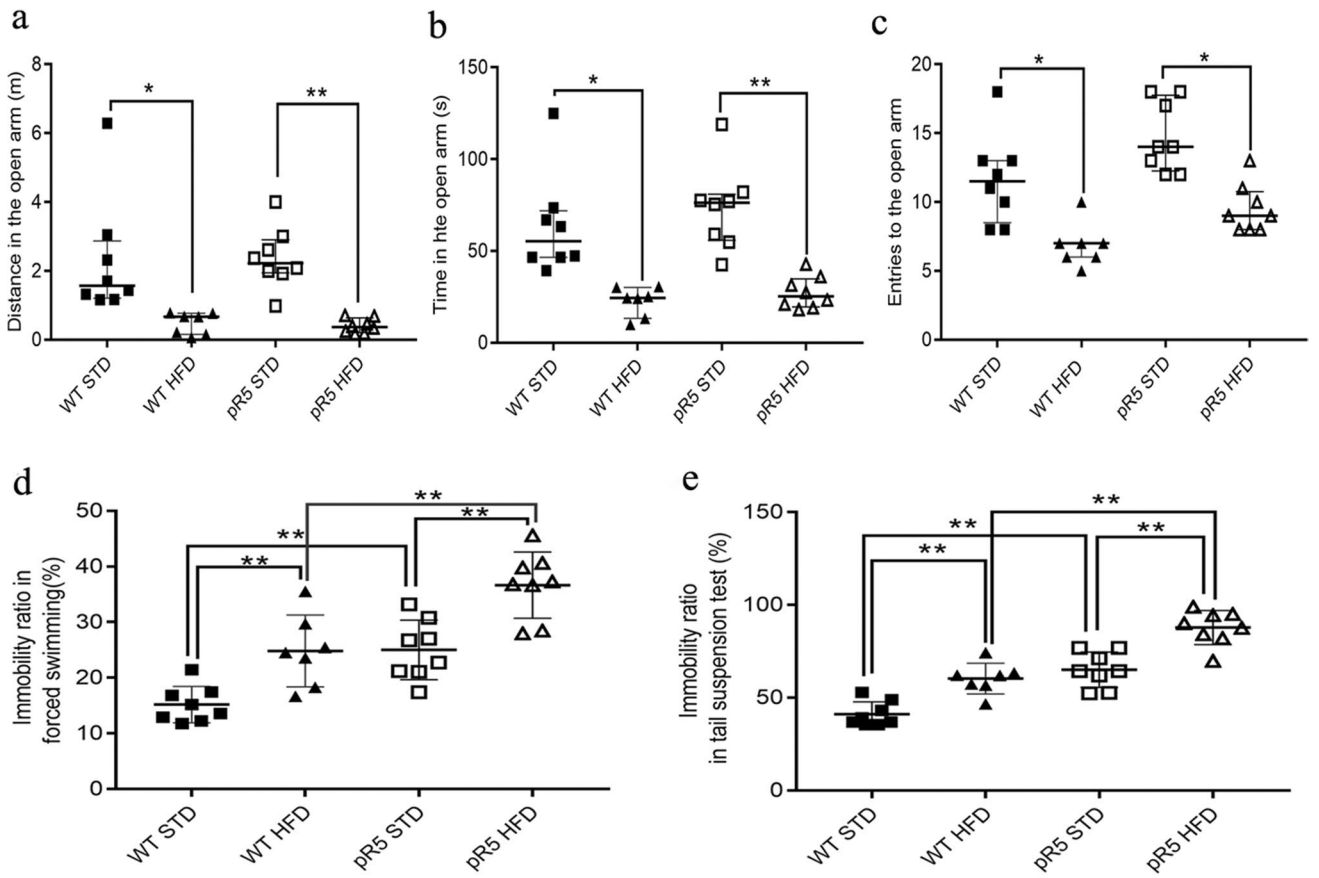

Fig. 2 Elevated plus-maze test (EPM), forced swim test (FST) and tail suspension test (TST). **a-c**. EPM. The values are presented as median and interquartile ranges, and between group comparisons were analyzed using the Kruskal–Wallis test followed by Dunn's test for post hoc analysis. **a**. Distance traveled in the open arms (Kruskal–Wallis test: χ^2 (3, N = 31) = 22.71, p < 0.001; Dunn's test, WT HFD vs. WT STD p = 0.015, pR5 HFD vs. pR5 STD p = 0.001). **b**. Time spent in the open arms (Kruskal–Wallis test: χ^2 (3, N = 31) = 22.35, p < 0.001; Dunn's test, WT HFD vs. WT STD p = 0.01, pR5 HFD vs. pR5 STD p = 0.003). **c**. Entries to the open arms (Kruskal–Wallis test: χ^2 (3, N = 31) = 20.21, p < 0.001; Dunn's test, WT HFD vs. WT STD p = 0.03, pR5 HFD vs. pR5 STD p = 0.04). **d-e**: FST and TST. The values are presented as mean ± S.D., and between group comparisons were analyzed using ANOVA post hoc test. **d**. Percentage immobility ratio in FST (one-way ANOVA, F [3, 27] = 21.54, p < 0.001; LSD test, WT HFD vs. WT STD p = 0.002, pR5 HFD vs. pR5 STD p < 0.001, WT HFD vs. pR5 HFD p < 0.001, WT STD vs. pR5 STD p = 0.001). **e**. Percentage immobility ratio in TST (one-way ANOVA, F [3, 27] = 40.51, p < 0.001; LSD test, WT HFD vs. WT STD p < 0.001, pR5 HFD vs. pR5 STD p < 0.001, WT HFD vs. pR5 HFD p < 0.001, WT STD vs. pR5 STD p < 0.001). *indicates p < 0.05, **indicates p < 0.01

a delayed glucose peak at 60 min after injection, while the glucose peak value for WT and pR5 STD groups was at 30 min after injection. Glucose levels at 120 min after glucose administration for WT and pR5 mice on HFD were still significantly higher while the glucose levels for WT and pR5 mice on STD decreased close to the fasting glucose levels. In addition, the mice on HFD had impaired glucose tolerance and this was potentiated by the genotype. The glucose levels in pR5 mice on the HFD at 15, 30, 60, 90 and 120 min were significantly higher compared to the corresponding WT mice on the STD (Fig. 1d).

Furthermore, we performed the ITT after 30 weeks of HFD to assess insulin sensitivity (Fig. 1e). Glucose levels for HFD and STD mice reached valley at 60 min after insulin injection and started to recover toward the baseline. However, glucose levels were significantly lower in the STD groups compared to the HFD groups at 15, 30, 60, 90 and 120 min after insulin injection. These results reveal impaired insulin sensitivity in the HFD groups. In addition, the glucose levels in pR5 HFD mice at 30, 60, 90 and 120 min were significantly higher compared to WT HFD mice (Fig. 1e), indicating that mice on HFD had impaired insulin sensitivity potentiated by the genotype.

WT and pR5 mice on HFD demonstrate increased anxiety like behavior in the elevated plus maze

Anxiety-like behavior was assessed in the elevated plus maze test, a well-established paradigm to assess anxiety related behavior in rodent models. Anxiety like behavior

was significantly increased in both pR5 and WT mice on HFD compared to the corresponding control groups on the STD as shown in Fig. 2a–c. Figure 2a illustrates that WT and pR5 mice on HFD traveled less distance in the open arms. Figure 2b shows HFD groups spent significantly less time in the open arms. Figure 2c shows HFD groups made fewer open arm entries. These measures varied significantly between STD and HFD mice, but there was no genotype effect between pR5 and WT mice.

pR5 mice on HFD demonstrate increased depression in the forced swim and tail suspension tests

Depression like behavior was assessed in the forced swim and tail suspension tests which measure the immobility time of the animals as a representation of behavioral despair. Depression like behavior was determined by the learned helplessness behavior in FST and TST.

The FST showed that both pR5 and WT mice on HFD had a significantly increased immobility time when compared with the mice on STD (Fig. 2d). In addition, the FST revealed a significant difference in immobility ratio between pR5 and WT genotypes. The immobility ratio for pR5 mice on STD was increased when compared with WT STD controls. Similarly, the immobility ratio for pR5 mice on HFD was increased when compared with their WT HFD controls, showing the greatest increase among the four groups.

The data from the TST had the same trend as the FST. A significant increase in percentage of immobility time was detected in WT and pR5 mice exposed to HFD (Fig. 2e) when compared with WT and pR5 mice fed with STD. Additionally, pR5 mice on STD showed increased immobility ratio when compared with WT mice on STD and this was potentiated in pR5 mice by HFD.

pR5 mice on HFD decrease recognition memory in the novel object recognition test

The novel object recognition test was used to evaluate the effect of HFD on the tendency of animals to explore novel objects over familiar objects. Results show a significant difference in the recognition index among groups. HFD significantly aggravated the recognition memory of WT and pR5 mice. Compared to their control littermates on STD, WT HFD mice and pR5 HFD mice showed a lower new object distance ratio, shorter new object time ratio and less new object entries. The pR5 HFD mice showed the worst interaction with the novel object among the groups, including object distance ratio (Fig. 3a), object time ratio (Fig. 3b) and new object entries (Fig. 3c).

Spatial reference memory deficits in pR5 mice

Morris's water maze (MWM) test is used to assess spatial reference learning and long-term memory. PR5 and WT mice were subjected to the MWM test to assess spatial reference memory. PR5 and WT mice on HFD, and their corresponding controls on the STD, learned to locate the hidden platform. This is indicated by decreases in escape latencies in the acquisition phase (Fig. 3d). The decrease in escape latencies was less pronounced in pR5 and WT mice on HFD compared to their controls on STD, indicating that the mice on HFD were much slower in learning the required task. In addition, the pR5 mice on the STD had higher escape latency compared with WT STD, while pR5 mice on the HFD had the highest escape latency. Additional measures such as time in the target quadrant (Fig. 3e) showed less improvement over four days of the test in pR5 and WT mice on HFD. PR5 mice spent less time in the target quadrant compared to WT indicating a genotypic effect (Fig. 3d). A further comparison revealed that pR5 mice on HFD spent less time in the target quadrant than the pR5 STD mice (Fig. 3e). Collectively, these findings indicate that pR5 mice have impaired learning which is aggravated by the HFD.

To test spatial reference memory of the former platform location (target quadrant), a probe trial was conducted. Compared to the pR5 and WT mice on the STD, pR5 and WT mice on HFD had significantly reduced time in the target quadrant (Fig. 3f), and reduced time spent in the platform zone (Fig. 3g). A significant difference was revealed between the genotypes. Compared to WT STD mice, pR5 STD mice had significantly reduced time in the target quadrant (Fig. 3f), and reduced time spent in the platform zone (Fig. 3g). When, compared to WT HFD mice, pR5 HFD mice had significantly reduced time in the target quadrant (Fig. 3g), and reduced time spent in the platform zone (Fig. 3g). In addition, the time in the target quadrant and time in the platform zone, were significantly decreased in pR5 mice on HFD compared to the other three groups. These results illustrate that pR5 mice have impaired reference memory, which is potentiated by the administration of HFD.

HFD increases total mouse tau, phosphorylated tau at Ser396 and Thr231 in pR5 and WT mice

To study the effect of long term HFD treatment on tau pathology, we performed immunostaining and western blotting of whole brain homogenates for phosphorylated tau at Ser396 and Thr231. Given the initial characterization of P301L mice, tau aggregates can be detected in several brain areas, early in the basolateral nucleus (BLA) of the amygdala and later in the hippocampus (< 18 months old) (Gotz et al. 2001; Pennanen et al. 2006).

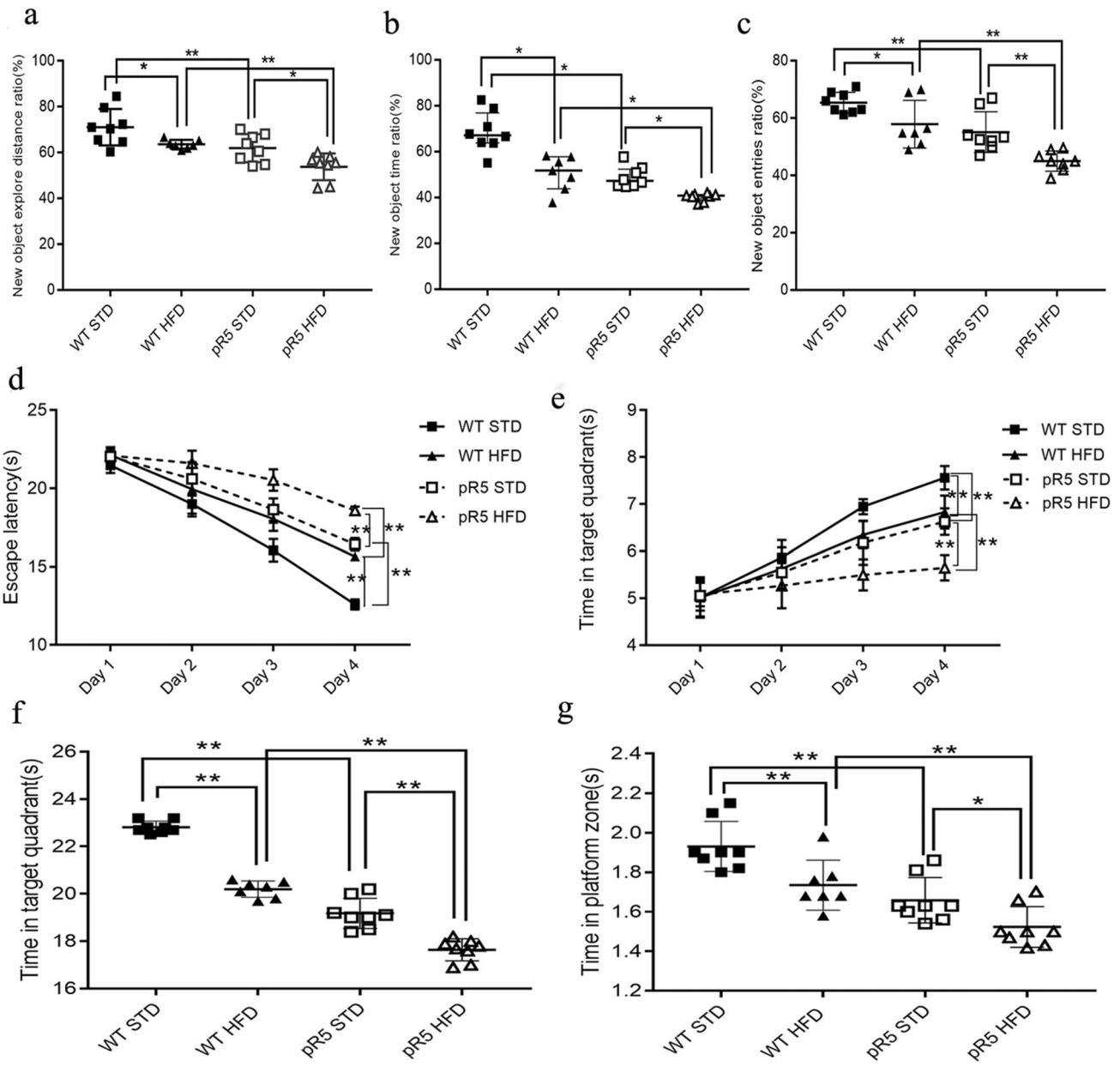

Fig. 3 New object recognition test and spatial reference memory in the Morris water maze. **a-c**: New object recognition test. **a**. New object explore distance ratio (one-way ANOVA, F [3, 27] = 11.194, $p < 0.001$; LSD test, WT HFD vs. WT STD $p = 0.023$, pR5 HFD vs. pR5 STD $p = 0.011$, WT STD vs. pR5 STD $p = 0.005$, WT HFD vs. pR5 HFD $p = 0.004$). **b**. New object explore time ratio (Kruskal–Wallis test: χ^2 (3, N = 31) = 22.68; Dunn's test: WT HFD vs. WT STD $p = 0.023$ pR5 HFD vs. pR5 STD $p = 0.028$, WT STD vs. pR5 STD $p = 0.011$, WT HFD vs. pR5 HFD $p = 0.020$). **c**. New object explore entries ratio (one-way ANOVA, F [3, 27] = 16.166, $p < 0.001$; LSD test, WT HFD vs. WT STD $p = 0.021$, pR5 HFD vs. pR5 STD $p = 0.002$, WT STD vs. pR5 STD $p = 0.002$, WT HFD vs. pR5 HFD $p < 0.001$). **d-e**: Acquisition learning in the MWM. The values are presented as mean ± S.D., and between group comparisons were analyzed using ANOVA post hoc test. **d**. Escape latency over 4 days of hidden platform test. Analysis for escape latency at day 4 of the hidden platform test, (one-way ANOVA, F [3, 27] = 363.11, $p < 0.001$; LSD test, WT HFD vs. WT STD $p < 0.001$, pR5 HFD vs. pR5 STD $p < 0.001$, WT HFD vs. WT HFD $p < 0.001$, WT STD vs. pR5 STD $p < 0.001$). **e**. Time spent in the target quadrant. Analysis for time spent in the target quadrant at day 4 of the hidden platform test, (one-way ANOVA, F [3, 27] = 66.86, $p < 0.001$; LSD test, WT HFD vs. WT STD $p < 0.001$, pR5 HFD vs. pR5 STD $p < 0.001$, WT HFD vs. WT HFD $p < 0.001$, WT STD vs. pR5 STD $p < 0.001$). **f-g**: Probe trial in MWM. The values are presented as mean ± S.D., and between group comparisons were analyzed using the ANOVA post hoc test. **f**. Time in the target quadrant (one-way ANOVA, F [3, 27] = 184.43, $p < 0.001$; LSD test, WT HFD vs. WT STD $p < 0.001$, pR5 HFD vs. pR5 STD $p < 0.001$, WT HFD vs. WT HFD $p < 0.001$, WT STD vs. pR5 STD $p < 0.001$). **g**. Time spent in the platform zone (one-way ANOVA, F [3, 27] = 16.61, $p < 0.001$; LSD test, WT HFD vs. WT STD $p = 0.003$, pR5 HFD vs. pR5 STD $p = 0.03$, WT HFD vs. pR5 HFD $p = 0.002$, WT STD vs. pR5 STD $p < 0.001$). * indicates $p < 0.05$, ** indicates $p < 0.01$

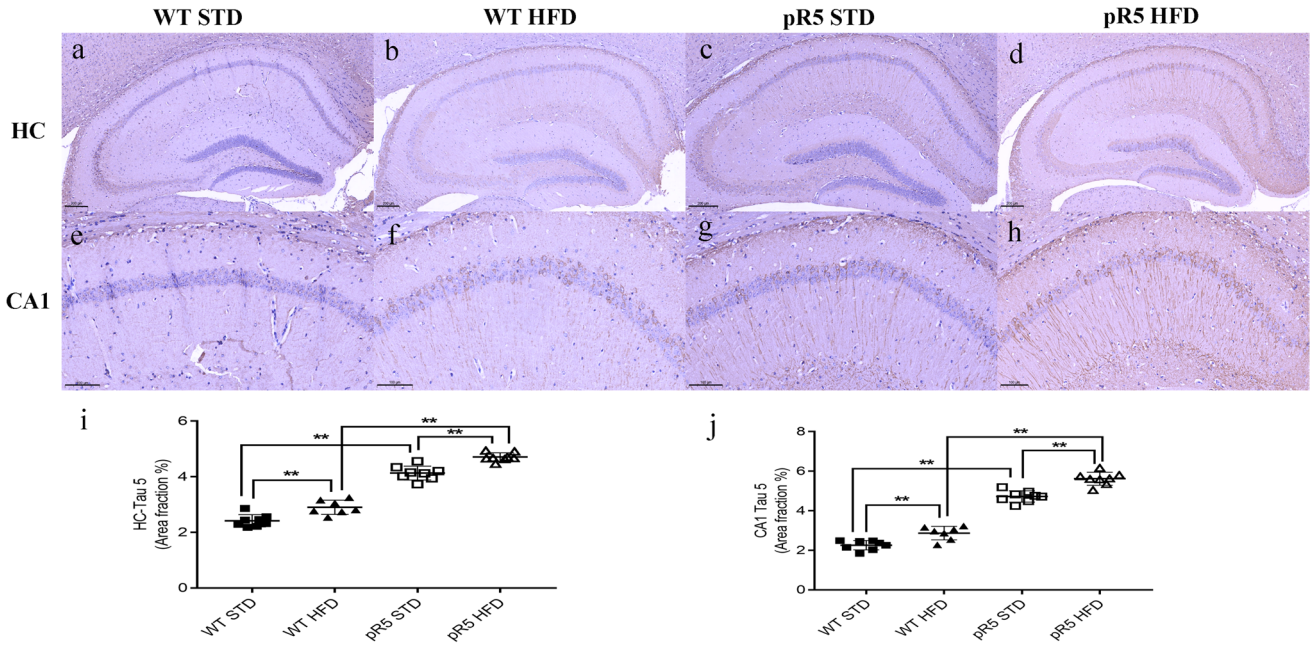

Fig. 4 Represents immunostaining of coronal hippocampus (HC) and CA1 region of HC brain section from pR5 mice and WT mice with anti-Tau 5. **a-d**. Images of the hippocampus immune-stained with anti-Tau 5 (Scale bar = 200 µm). **e-h**. Images of CA1 region of the hippocampus immune-stained with anti-Tau 5 (Scale bar = 100 µm). **i** and **j** are representative quantification (% of area fraction) of Tau 5 expression levels in hippocampus and CA1 regions, showing that HFD treatment significantly increased the levels of Tau 5 in the hippocampus and CA1 regions, with highest Tau 5 immunostaining in the pR5 mice on HFD. Results are presented as mean ± S.D. (Tau 5 expression levels in HC: one-way ANOVA, F [3, 27] = 179.896, $p < 0.001$; LSD test, WT HFD vs. WT STD $p < 0.001$, pR5 HFD vs. pR5 STD $p < 0.001$, WT STD vs. pR5 STD $p < 0.001$, WT HFD vs. pR5 HFD $p < 0.001$. Tau 5 expression in CA1 region: one-way ANOVA, F [3, 27] = 213.793, $p < 0.001$; LSD test, WT HFD vs. WT STD $p = 0.001$, pR5 HFD vs. pR5 STD $p < 0.001$, WT STD vs. pR5 STD $p < 0.001$, WT HFD vs. pR5 HFD $p < 0.001$). *indicates $p < 0.05$, **indicates $p < 0.01$

IHC revealed that HFD treatment significantly increased the immunoreactivity of Tau 5 (Fig. 4), p (Ser396)-tau (Fig. 5) and p (Thr231)-tau (Fig. 6) in the amygdala and hippocampus CA1 compared to controls. Western blot analysis showed a significant increase in the levels of total tau protein (tau 5) and phosphorylated tau protein in the brains of P301L and WT HFD mice, when compared to WT STD mice. The levels of p (Thr231)-tau and p (Ser396)-tau were significantly increased in both pR5 and WT mice treated with HFD compared to STD treatment groups respectively (Fig. 7). Furthermore, it is worth mentioning that the pR5 mice showed higher total tau protein and hyperphosphorylated tau at epitope Ser396 and Thr231 (Fig. 7). Interestingly, our results suggest that long term HFD may increase total and hyperphosphorylated tau in WT mice. HFD also aggravates tau hyperphosphorylation in pR5 transgenic mice. Full western blots showing the marker are included in the supplement 2.

Discussion

In the present study, we investigated the effect of long term HFD on P301L and wild type mice. We aimed to evaluate changes in peripheral insulin resistance, cognitive behavior, and tau pathology following 30 weeks HFD treatment. We report the establishment of a P301L transgenic mouse model with combined peripheral insulin resistance and tau pathology. Our results show that HFD facilitates the development of peripheral insulin resistance and augments cognitive behavior changes, and tau pathology in pR5 transgenic mice. The possible consequence of HFD-induced pathological changes is ultimately, an aggravation of cognitive deficits in these mice.

The increased prevalence of the often-associated chronic obesity and T2DM is largely driven by excessive energy intake, which is a product of both the amount, and caloric density of food consumed. Obesity and T2DM together, are linked to impaired central nervous system (CNS) function, and are highly associated with Alzheimer disease (AD), which is also increasing in prevalence.

In the present study, MAPT P301L (pR5 strain) transgenic mice gradually develop phosphorylated tau protein similar to humans in the CA1 area of the hippocampus, amygdala, and frontal lobe of the brain from about 6 months old, forming NFT's and showing abnormal mental behavior, and impairment of spatial learning ability (Bodea et al. 2017; Gotz et al. 2001). The administration of HFD closely mimics the ready availability of high fat,

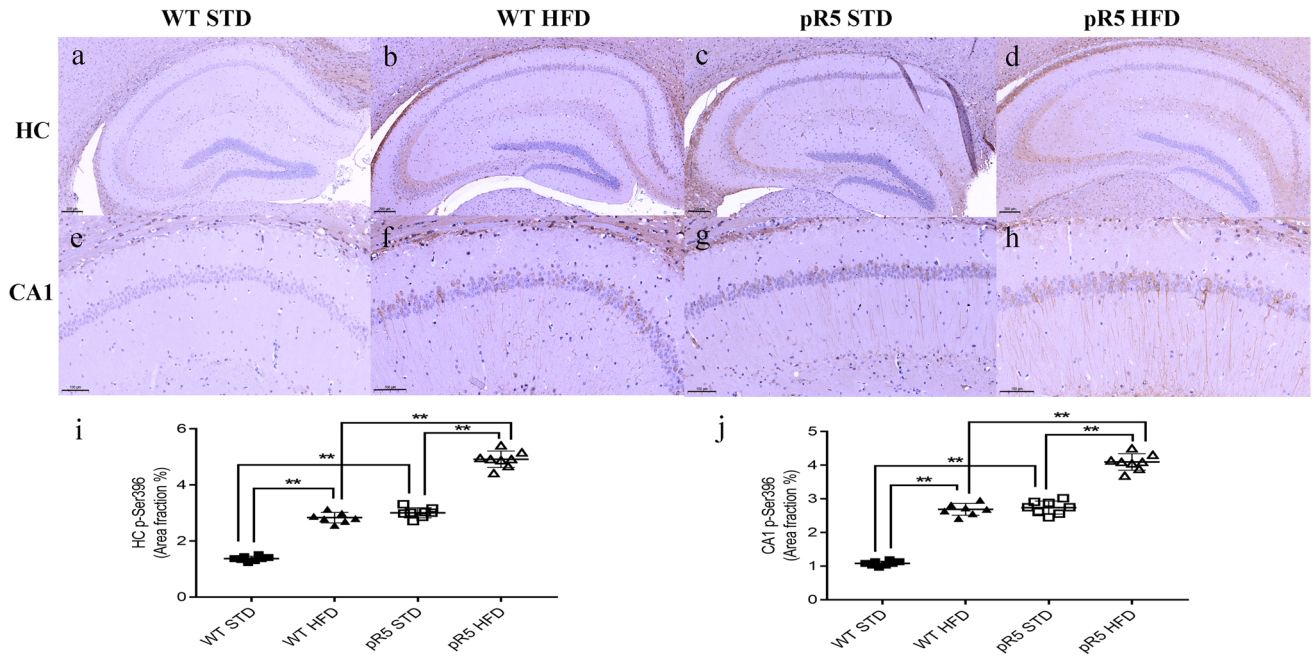

Fig. 5 Represents immunostaining of coronal hippocampus (HC) and CA1 region of HC brain section from pR5 mice and WT mice with anti-p (Ser 396)-tau. **a-d**. Images of the hippocampus immune-stained with anti-p (Ser396)-tau (Scale bar = 200 µm). **e-h**. Images of CA1 region of the hippocampus immune-stained with anti-p (Ser396)-tau (Scale bar = 100 µm). **i**. and **j**. are representative quantification (% of area fraction) of p (Ser396)-tau expression levels in hippocampus and CA1 regions, showing that HFD treatment significantly increased the levels of p (Ser396)-tau in the hippocampus and CA1 regions, with highest p (Ser396)-tau immunostaining in the pR5 mice on HFD. Results are presented as mean ± S.D.(p(Ser396)-tau expression levels in HC: one-way ANOVA, $F[3, 27] = 594.93$, $p < 0.001$; LSD test, WT HFD vs. WT STD $p < 0.001$, pR5 HFD vs. pR5 STD $p < 0.001$, WT STD vs. pR5 STD $p < 0.001$, WT HFD vs. pR5 HFD $p < 0.001$. p (Ser396)-tau expression levels in CA1 region: one-way ANOVA, $F[3, 27] = 366.516$, $p < 0.001$; LSD test, WT HFD vs. WT STD $p < 0.001$, pR5 HFD vs. pR5 STD $p < 0.001$, WT STD vs. pR5 STD $p < 0.001$, WT HFD vs. pR5 HFD $p < 0.001$). *indicates $p < 0.05$, **indicates $p < 0.01$

energy dense foods of modern society, which is the main contributor to the obesity trend in human populations. Therefore, we adopted high fat diet feeding of pR5 mice from the age of 2 months to the age of 9 months, the age when, according to previous studies, tau pathology has been established, and mice show cognitive decline (Bodea et al. 2017; Gotz et al. 2001).

We evaluated changes to the metabolic and behavioral parameters of this transgenic model under a HFD feeding regimen. As expected, HFD drastically increased the weight of the animals regardless of the genotype. In accordance with a previous study (Bodea et al. 2017), energy intake was increased in HFD fed mice compared with STD mice throughout the study period. After an initial increase, energy intake was consistently higher after 4 weeks in the HFD treatment groups, with the difference between HFD groups and STD groups being stable. As indicated in a previous study (Bodea et al. 2017), as caloric intake declined, weight gain continued, indicating that metabolic efficiency was reduced in the HFD fed mice (Winzell and Ahren 2004; Yang et al. 2014). The energy intake pattern was similar in WT and pR5 HFD mice, with a larger caloric intake in pR5 HFD mice throughout the experiment.

The growth curve patterns are individually similar in HFD fed groups, and STD fed groups respectively. There was a slight increase in energy intake and body weight of pR5 on STD, when compared to WT mice on STD, with no significant difference between the groups. During the first two weeks following introduction of the HFD, body weight increased significantly more in the HFD fed mice than in STD fed mice. The weight gain continued thereafter to be progressively higher in HFD mice. PR5 mice had a higher energy intake throughout the experiment as they were prone to eat more than WT. There was a higher body weight gain in pR5 HFD mice after 4 weeks HFD feeding, continuing thereafter to be progressively higher in pR5 HFD mice when compared with WT HFD mice. Significant augmented growth was observed in pR5 HFD fed mice from 18 weeks (at the age of 26 weeks), when tau pathology has been established in P301L mice according to a previous study (Bodea et al. 2017; Gotz et al. 2001). Collectively, our data indicates that pR5 mice fed with HFD are more vulnerable

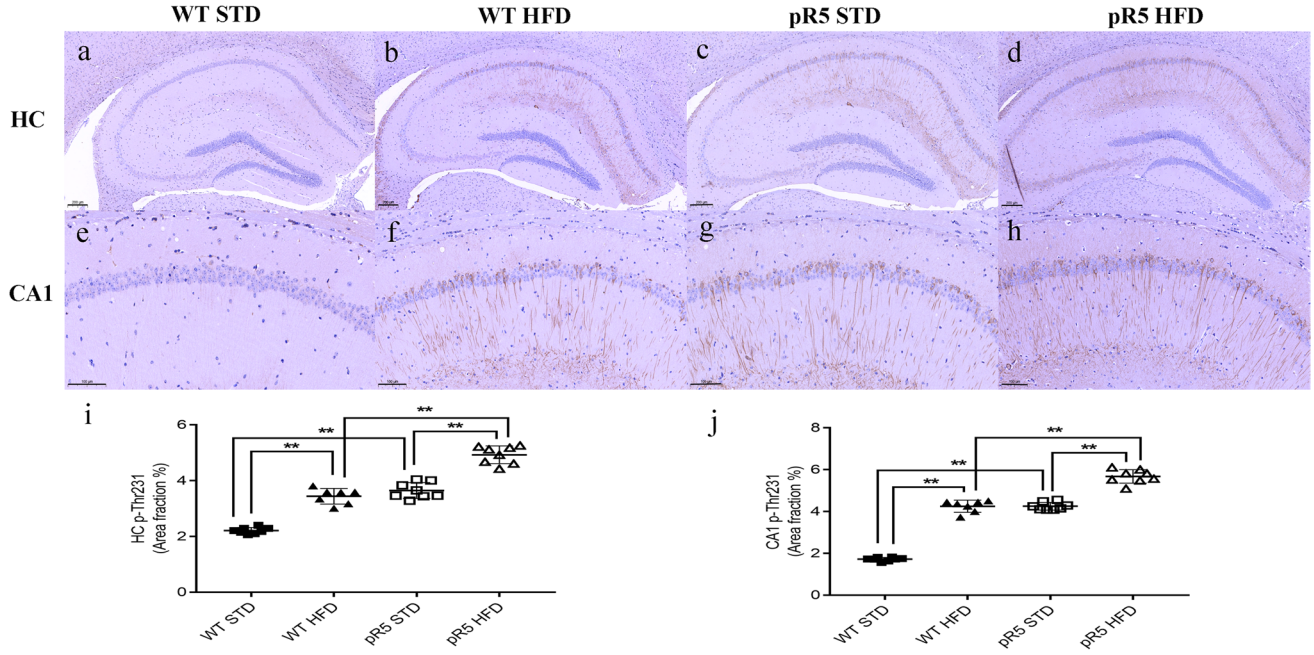

Fig. 6 Represents immunostaining of coronal hippocampus (HC) and CA1 region of HC brain section from pR5 mice and WT mice with anti-p (Thr231)-tau. **a-d**. Images of the hippocampus immune-stained with anti-p (Thr231)-tau (Scale bar = 200 µm). **e-h**. Images of CA1 region of the hippocampus immune-stained with anti-p (Thr231)-tau (Scale bar = 100 µm). **i** and **j** are representative quantification (% of area fraction) of p (Thr231)-tau expression levels in hippocampus and CA1 regions, showing that HFD treatment significantly increased the levels of p (Thr231)-tau in the hippocampus and CA1 regions, with highest p (Thr231)-tau immunostaining in the pR5 mice on HFD. Results are presented as median and interquartile ranges, a non-parametric Kruskal–Wallis test was used, followed by Dunn's test for post hoc analysis. P (Thr231)-tau expression levels in HC: Kruskal–Wallis test: χ^2 (3, N = 31) = 25.94; Dunn's test: WT HFD vs. WT STD p = 0.032, pR5 HFD vs. pR5 STD p = 0.024, WT STD vs. pR5 STD p = 0.005, WT HFD vs. pR5 HFD p = 0.006. p (Thr231)-tau expression in CA1 region: Kruskal–Wallis test: χ^2 (3, N = 31) = 25.63; Dunn's test: WT HFD vs. WT STD p = 0.012, pR5 HFD vs. pR5 STD p = 0.01, WT STD vs. pR5 STD p = 0.013, WT HFD vs. pR5 HFD p = 0.017). * indicates p < 0.05, ** indicates p < 0.05

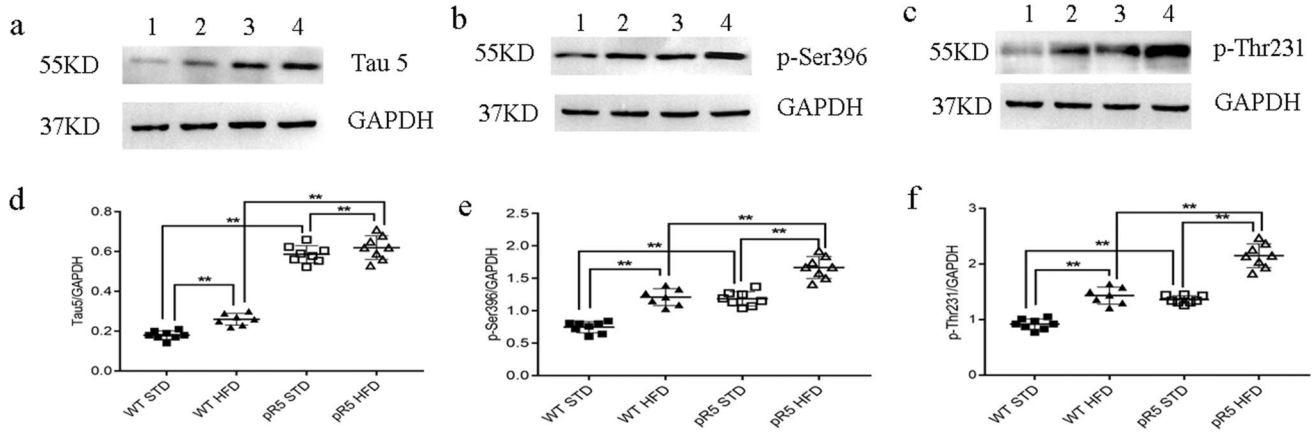

Fig. 7 HFD aggravates tau hyperphosphorylation in P301L mice and WT mice. The values are presented as mean ± S.D., and between group comparisons were analyzed using the ANOVA post hoc test. **a-c**. Represents Tau immunostaining (identified by Tau 5, p (Ser396)-tau and p (Thr231)-tau respectively; 1, 2, 3, 4 bands represent WT STD, WT HFD, pR5 STD and pR5 HFD groups respectively). **d**. Immunoblot analysis of Tau 5 (Tau 5/GAPDH: one-way ANOVA, F [3, 27] = 180.11, p < 0.001; LSD test: WT HFD vs. WT STD p = 0.002, WT HFD vs. pR5 HFD p < 0.001, WT STD vs. pR5 STD p < 0.001). **e**. Immunoblot analysis of p (Ser396)- tau (p-Ser396 / GAPDH: one-way ANOVA, F [3, 27] = 109.41, p < 0.001; LSD test: pR5 HFD vs. pR5 STD p = < 0.001, WT HFD vs. WT STD p < 0.001, WT HFD vs. WT HFD p < 0.001). **f**. Immunoblot analysis of p (Thr231)-tau (p-Thr231/GAPDH: one-way ANOVA, F [3, 27] = 116.06, p < 0.001; LSD test: pR5 HFD vs. pR5 STD p < 0.001, WT HFD vs. WT STD p < 0.001, WT HFD vs. pR5 HFD p < 0.001). **indicates p < 0.01

to diet induced obesity compared to WT, especially with increasing age.

The baseline fasting blood glucose levels were not different between all the groups but after 4 weeks of HFD, higher glucose levels were established in WT and pR5 mice on HFD compared to the mice on STD. The increased blood glucose levels at 4 weeks coincided with increased food intake and body weight. The blood glucose levels in the HFD groups continued to increase progressively until 16 weeks, and were then stable throughout the remaining weeks of the treatment period. The GTT revealed a marked deterioration of glucose elimination in WT and pR5 mice on HFD, and this was likely due to the reduction of insulin sensitivity as shown by the ITT. Hence, HFD can accelerate the onset, and increase the severity of obesity and glucose metabolism disorders in pR5 and WT mice.

Based on the time course of the GTT and ITT, it appears that glucose elimination and insulin sensitivity are worse in pR5 HFD compared to WT HFD. The pR5 mice on HFD had aggravated deterioration in glucose elimination and insulin sensitivity impairment compared to WT on HFD. It has been found in a recent study that phosphorylated tau protein is related to insulin resistance and glucose metabolism balance in the brain and periphery. Our findings allude to the importance of tau pathology in the potentiation of metabolic disorders.

The pR5 mouse line overexpresses the P301L mutation using the longest human tau isoform under the control of the neuron specific mouse Thy1.2 promoter (Gotz et al. 2001). In these mice, pronounced tau hyperphosphorylation, resulting in NFT formation, is initiated in the amygdala at around 6 months of age and subsequently in the CA1 region of the hippocampus (Pennanen et al. 2006). Impaired function of the amygdala is associated with anxiety and depression while impaired hippocampal function is associated with anxiety and memory dysfunction (Cavedo et al. 2014; Pennanen et al. 2006; Poulin et al. 2011).

We assessed the impact of high fat diet on amygdala and hippocampal dependent tasks such as anxiety, depression, and memory in P301L tau transgenic mice. In our study, a significant dietary effect was detected in measures of anxiety like behavior in the elevated plus maze test between HFD and STD mice such as reduced distance traveled, and less time and entries in the open arms. These findings are in accordance with observations reported in recent studies, that chronic consumption of high fat food leads to anxiety like behaviors in mice (Andre et al. 2014; Aslani et al. 2015; Dutheil et al. 2016).

In addition, we observed that HFD induced depression like behavior in WT and pR5 mice, signified by increased immobility in the FST and TST behavioral tests. A recent study showed that mice fed with HFD for 14 weeks had increased immobility time in the FST which is consistent with our findings (Kurhe et al. 2014). It is reported that obese individuals have about a 55% increased risk of developing depression, whereas diabetes is estimated to double the incidence of depression (Anderson et al. 2001; Luppino et al. 2010).

Furthermore, we noticed that pR5 mice on STD had increased immobility time in the FST and TST compared with the WT mice on STD indicating a genotype effect on depression like behavior in pR5 mice (Baumeister and Harter 2007; John et al. 2005). The depression like behavior was most prominent in pR5 mice on HFD. These findings show that HFD augments depression like behavior in pR5 mice, indicating that pR5 mice are more prone to HFD induced depression. Notably, it is reported that depressed individuals are more likely to gain excessive weight due to reduced energy metabolism (Luppino et al. 2010; Macht 2008). Based on our results and other studies, obesity and diabetes increase the risk of developing depression, and depression increases the risk of developing obesity and diabetes.

From our study, depression in HFD mice might contribute substantially to increased food consumption and the burden of metabolic disorders, with greater effect in pR5 mice than WT. As pR5 mice are already prone to depression due to tau pathology, feeding them HFD augments their depression as they become obese and develop diabetes, having a greater effect than on WT.

Our assessment of cognitive function using MWM tests, show that diabetes and obesity induced by HFD are associated with cognitive impairment in pR5 and WT mice. Based on impaired acquisition learning in MWM tests,pR5 and WT mice on HFD had less reduced latency time and less increased time in the target quadrant in the acquisition learning test, indicating impaired learning ability after long term HFD. From the probe test, pR5 and WT mice on HFD spent less time in the designated platform quadrant, indicating impairment in spatial reference memory compared to controls on STD. The observed deficits in spatial reference memory in pR5 mice may be due to aggregation of tau in the hippocampus and the basolateral amygdala (BLA) (Pennanen et al. 2006; Roozendaal et al. 2003). Notably, pR5 HFD mice had the poorest spatial reference memory among the groups, therefore, the presence of T2DM aggravates the impairment of spatial reference memory in pR5 mice.

Insulin resistance, is considered a hallmark of T2DM and obesity might directly influence the pathology and behavioral characteristics of not only metabolic diseases, but also psychiatric and neurodegenerative diseases. These alterations include changes in dopamine signaling, blood–brain barrier function, hippocampal synaptic plasticity, mitochondrial function, and expression of amyloid β and microtubule associated tau protein (Schubert et al. 2004). Clinical research reports that patients with type 2 diabetes are insulin resistant for many years before their diagnosis, which

can negatively affect the brain, with the effect of T2DM on cognitive function obvious in elderly people (Biessels and Despa 2018; Kullmann et al. 2020).

Aβ amyloid plaques, and neurofibrillary tangles (NFT's), are aggregates of hyperphosphorylated tau, and are the major pathological hallmarks of AD. The pR5 mouse line overexpresses the P301L mutation which leads to pronounced hyperphosphorylated tau at multiple sites, including T181 (AT270), AT8, T212/S214 (AT100), S262/S356 (12E8), and S396/S404 (PHF-1). They are initially detected in the amygdala and subsequently in the CA1 region of the hippocampus, resulting in behavioral impairments in amygdala and hippocampus-dependent functions (Ke et al. 2009).

Given their link to AD, hyperphosphorylated tau, insulin-dependent glycogen synthesis and behavioral impairments, we performed immunostaining and western blotting to assess total tau and phosphorylated tau at sites Ser396 and Thr231 in pR5 and WT mice on HFD compared to STD controls.

Recently, p (Thr231)-tau has been detected to be elevated in CSF of patients with AD. For identifying patients with AD, p (Thr231)-tau may have better sensitivity than p (Thr181)-tau, with less false positives (Xia et al. 2021). Previous results suggest that phosphorylation of Thr231 and Ser396 by GSK3β may play an important role in hyperphosphorylation of tau and insulin-dependent glycogen synthesis (Lin et al. 2007). A recent study demonstrated that phosphorylated tau at sites Ser 396/404 is increased in the hippocampus of aged mice, coinciding with observed oxidative damage and mitochondrial dysfunction, contributing to synaptic failure and memory loss at an advanced age (Torres et al. 2021). Experimental DM was induced by administration of streptozotocin (STZ), which causes insulin deficiency and increased phosphorylation of endogenous murine tau at the Ser396 site in the amygdala (Ke et al. 2009). We investigated the effect of long term HFD on tau pathology in the brains of WT and P301L mice by performing western blotting of whole brain homogenates for total tau, phosphorylated tau at sites Ser396 and Thr231.

Western blot analysis showed a significant increase in the levels of total tau protein (Tau 5) and phosphorylated tau protein in the brains of P301L and WT HFD mice, when compared to WT STD mice. The levels of p-Thr231 and p-Ser396 were significantly increased in both pR5 and WT mice treated with HFD compared to STD treatment groups respectively. Furthermore, it is worth mentioning that the P301L mice showed higher total tau protein, and hyperphosphorylated tau at sites Ser396 and Thr231. Interestingly, our results suggest that long term HFD may increase total and hyperphosphorylated tau in WT mice. HFD also aggravates tau hyperphosphorylation in pR5 transgenic mice.

In our present study, as in previous reports, HFD is a diabetogenic agent that induces obesity, insulin resistance and T2DM, which mimics the T2DM patients who develop from obesity and insulin resistance due to the long term high fat diet of modern society. Mice in our study were treated with long term HFD through to older age. As we expected, HFD impacted negatively on both memory and learning functions in P301L mice and WT mice at the age of 9 months. Western blotting of total brain homogenates revealed that HFD treatment significantly increases the immunoreactivity of total tau, p (Ser396)-tau and p (Thr231)-tau in pR5 and WT mice, compared to STD controls. In the same context, western blotting showed greatest increase in the expression levels of total tau and p (Ser396)-tau in pR5 HFD mice. We believe that the effect of HFD was significant at advanced ages in this model, and became more obvious in P301L transgene mice as a result of tau pathology aggravation. Hyperphosphorylated tau protein is one of the important pathological changes of AD, and correlates with the severity of dementia. Moreover, hyperphosphorylated tau is also found in other degenerative brain diseases, such as frontotemporal dementia and Huntington's disease (Gong et al. 2016). Hence, HFD can accelerate the onset, and increase the severity of obesity and glucose metabolism disorders in individuals with a predisposition to developing tau pathology.

It is worth noting, as shown in our study, pR5 and WT mice fed HFD presented with insulin resistance. While it was more obvious in pR5 HFD mice, pR5 STD mice also showed impairment of insulin function at the age of 9 months, when pR5 mice are shown to have developed cognitive impairment and tau pathology in the brain. Several clinical studies provide evidence of a bidirectional relationship between metabolic disease and cognitive impairments forming a vicious circle. However, the exact underlying mechanisms are not fully understood. For example, patients with AD and schizophrenia have reduced peripheral insulin sensitivity (Ghasemi et al. 2013; Kullmann et al. 2020).

The P301L-HFD mouse model presents that peripheral insulin resistance and cognitive impairment with hyperphosphorylated tau in the brain, could reflect the interaction between genetic and etiologic factors of AD and other tauopathies. This will help us to explore possible underlying mechanisms for bidirectional relationships between T2DM or insulin resistance and cognitive impairment.

In conclusion, our results support the relationship between HFD induced metabolic disorders and AD. HFD promotes cognitive impairment, anxiety, and depression like behavior in both WT and pR5 mice. HFD induces diabetes and obesity, and aggravates cognitive impairment and depressive like behavior in P301L tau transgenic mice.

The data presented herein are of particular relevance in the context of the current obesity epidemic, highlighting the impact of HFD induced obesity and diabetes on AD, and illustrating the effects of metabolic disorders and tauopathies on mood and cognitive function.

This model is therefore, suitable for studying the underlying biochemical changes and mechanisms associated with metabolic disorders and AD tauopathy, and for the development of therapeutics and treatments for these debilitating conditions.

Supplementary Information The online version contains supplementary material available at https://doi.org/10.1007/s11011-022-01029-x.

Acknowledgements We thank and acknowledge Dr. Mohammed Al-Hawwas for training and help with mouse genotyping.

All authors critically reviewed content and approved final version for publication.

Author contributions Xin-Fu Zhou was responsible for the study concept and design. Jing Xiong contributed to the animal work, data analysis and interpretation of findings. Issac Deng, Sally Kelliny, and Liying Lin assisted with animal work. Jing Xiong drafted the manuscript, Xin-Fu Zhou provided critical revision of the manuscript and Larisa Bobrovskaya supervised students involved.

Funding This work was supported by grants from NHMRC APP1020567, Chinese CSC 2011CB944200, Discipline leader program of Yunnan Province D-2017028 and Research program of Health Commission of Yunnan Province 2017NS287.

Data availability The authors declare that data will be made available upon reasonable request.

Declarations

Conflict of interest The authors declare that they have no conflicts of interest in this study.

References

Anderson RJ, Freedland KE, Clouse RE, Lustman PJ (2001) The prevalence of comorbid depression in adults with diabetes: a meta-analysis. Diabetes Care 24:1069–1078. https://doi.org/10.2337/diacare.24.6.1069

Andre C, Dinel AL, Ferreira G, Laye S, Castanon N (2014) Diet-induced obesity progressively alters cognition, anxiety-like behavior and lipopolysaccharide-induced depressive-like behavior: focus on brain indoleamine 2,3-dioxygenase activation. Brain Behav Immun 41:10–21. https://doi.org/10.1016/j.bbi.2014.03.012

Andrikopoulos S, Blair AR, Deluca N, Fam BC, Proietto J (2008) Evaluating the glucose tolerance test in mice. Am J Physiol Endocrinol Metab 295:E1323–E1332. https://doi.org/10.1152/ajpendo.90617.2008

Aslani S, Vieira N, Marques F, Costa PS, Sousa N, Palha JA (2015) The effect of high-fat diet on rat's mood, feeding behavior and response to stress. Transl Psychiatry 5:e684. https://doi.org/10.1038/tp.2015.178

Bandosz P, Ahmadi-Abhari S, Guzman-Castillo M, Pearson-Stuttard J, Collins B, Whittaker H, Shipley MJ, Capewell S, Brunner EJ, O'Flaherty M (2020) Potential impact of diabetes prevention on mortality and future burden of dementia and disability: a modelling study. Diabetologia 63:104–115. https://doi.org/10.1007/s00125-019-05015-4

Baumeister H, Harter M (2007) Mental disorders in patients with obesity in comparison with healthy probands. Int J Obes (Lond) 31:1155–1164. https://doi.org/10.1038/sj.ijo.0803556

Belovicova K, Bogi E, Csatlosova K, Dubovicky M (2017) Animal tests for anxiety-like and depression-like behavior in rats. Interdiscip Toxicol 10:40–43. https://doi.org/10.1515/intox-2017-0006

Biessels GJ, Despa F (2018) Cognitive decline and dementia in diabetes mellitus: mechanisms and clinical implications. Nat Rev Endocrinol 14:591–604. https://doi.org/10.1038/s41574-018-0048-7

Bodea LG, Evans HT, Van der Jeugd A, Ittner LM, Delerue F, Kril J, Halliday G, Hodges J, Kiernan MC, Gotz J (2017) Accelerated aging exacerbates a pre-existing pathology in a tau transgenic mouse model. Aging Cell 16:377–386. https://doi.org/10.1111/acel.12565

Cavedo E, Pievani M, Boccardi M, Galluzzi S, Bocchetta M, Bonetti M, Thompson PM, Frisoni GB (2014) Medial temporal atrophy in early and late-onset Alzheimer's disease. Neurobiol Aging 35:2004–2012. https://doi.org/10.1016/j.neurobiolaging.2014.03.009

Clodfelder-Miller BJ, Zmijewska AA, Johnson GV, Jope RS (2006) Tau is hyperphosphorylated at multiple sites in mouse brain in vivo after streptozotocin-induced insulin deficiency. Diabetes 55:3320–3325. https://doi.org/10.2337/db06-0485

Dutheil S, Ota KT, Wohleb ES, Rasmussen K, Duman RS (2016) High-fat diet induced anxiety and anhedonia: impact on brain homeostasis and inflammation. Neuropsychopharmacology 41:1874–1887. https://doi.org/10.1038/npp.2015.357

Ellacott KL, Morton GJ, Woods SC, Tso P, Schwartz MW (2010) Assessment of feeding behavior in laboratory mice. Cell Metab 12:10–17. https://doi.org/10.1016/j.cmet.2010.06.001

Freude S, Plum L, Schnitker J, Leeser U, Udelhoven M, Krone W, Bruning JC, Schubert M (2005) Peripheral hyperinsulinemia promotes tau phosphorylation in vivo. Diabetes 54:3343–3348. https://doi.org/10.2337/diabetes.54.12.3343

Ghasemi R, Dargahi L, Haeri A, Moosavi M, Mohamed Z, Ahmadiani A (2013) Brain insulin dysregulation: implication for neurological and neuropsychiatric disorders. Mol Neurobiol 47:1045–1065. https://doi.org/10.1007/s12035-013-8404-z

Goncalves RA, Wijesekara N, Fraser PE, De Felice FG (2019) The link between tau and insulin signaling: implications for Alzheimer's disease and other tauopathies. Front Cell Neurosci 13:17. https://doi.org/10.3389/fncel.2019.00017

Gong CX, Liu F, Iqbal K (2016) O-GlcNAcylation: A regulator of tau pathology and neurodegeneration. Alzheimers Dement 12:1078–1089. https://doi.org/10.1016/j.jalz.2016.02.011

Gotz J, Chen F, Barmettler R, Nitsch RM (2001) Tau filament formation in transgenic mice expressing P301L tau. J Biol Chem 276:529–534. https://doi.org/10.1074/jbc.M006531200

Hryhorczuk C, Sharma S, Fulton SE (2013) Metabolic disturbances connecting obesity and depression. Front Neurosci 7:177. https://doi.org/10.3389/fnins.2013.00177

John U, Meyer C, Rumpf HJ, Hapke U (2005) Relationships of psychiatric disorders with overweight and obesity in an adult general population. Obes Res 13:101–109. https://doi.org/10.1038/oby.2005.13

Jolivalt CG, Lee CA, Beiswenger KK, Smith JL, Orlov M, Torrance MA, Masliah E (2008) Defective insulin signaling pathway and increased glycogen synthase kinase-3 activity in the brain of diabetic mice: parallels with Alzheimer's disease and correction by insulin. J Neurosci Res 86:3265–3274. https://doi.org/10.1002/jnr.21787

Kandimalla R, Thirumala V, Reddy PH (2017) Is Alzheimer's disease a Type 3 Diabetes? A critical appraisal. Biochim Biophys Acta Mol Basis Dis 1863:1078–1089. https://doi.org/10.1016/j.bbadis.2016.08.018

Kanoski SE, Davidson TL (2011) Western diet consumption and cognitive impairment: links to hippocampal dysfunction and obesity. Physiol Behav 103:59–68. https://doi.org/10.1016/j.physbeh.2010.12.003

Ke YD, Delerue F, Gladbach A, Gotz J, Ittner LM (2009) Experimental diabetes mellitus exacerbates tau pathology in a transgenic mouse model of Alzheimer's disease. PLoS ONE 4:e7917. https://doi.org/10.1371/journal.pone.0007917

Kelliny S, Lin L, Deng I, Xiong J, Zhou F, Al-Hawwas M, Bobrovskaya L, Zhou XF (2021) A new approach to model sporadic Alzheimer's disease by intracerebroventricular streptozotocin injection in APP/PS1 mice. Mol Neurobiol 58:3692–3711. https://doi.org/10.1007/s12035-021-02338-5

Kullmann S, Heni M, Hallschmid M, Fritsche A, Preissl H, Haring HU (2016) Brain insulin resistance at the crossroads of metabolic and cognitive disorders in humans. Physiol Rev 96:1169–1209. https://doi.org/10.1152/physrev.00032.2015

Kullmann S, Kleinridders A, Small DM, Fritsche A, Haring HU, Preissl H, Heni M (2020) Central nervous pathways of insulin action in the control of metabolism and food intake. Lancet Diabetes Endocrinol 8:524–534. https://doi.org/10.1016/S2213-8587(20)30113-3

Kurhe Y, Radhakrishnan M, Gupta D (2014) Ondansetron attenuates depression co-morbid with obesity in obese mice subjected to chronic unpredictable mild stress; an approach using behavioral battery tests. Metab Brain Dis 29:701–710. https://doi.org/10.1007/s11011-014-9574-8

Lin YT, Cheng JT, Liang LC, Ko CY, Lo YK, Lu PJ (2007) The binding and phosphorylation of Thr231 is critical for Tau's hyperphosphorylation and functional regulation by glycogen synthase kinase 3beta. J Neurochem 103:802–813. https://doi.org/10.1111/j.1471-4159.2007.04792.x

Liu Y, Liu F, Grundke-Iqbal I, Iqbal K, Gong CX (2011) Deficient brain insulin signalling pathway in Alzheimer's disease and diabetes. J Pathol 225:54–62. https://doi.org/10.1002/path.2912

Luppino FS, de Wit LM, Bouvy PF, Stijnen T, Cuijpers P, Penninx BW, Zitman FG (2010) Overweight, obesity, and depression: a systematic review and meta-analysis of longitudinal studies. Arch Gen Psychiatry 67:220–229. https://doi.org/10.1001/archgenpsychiatry.2010.2

Macht M (2008) How emotions affect eating: a five-way model. Appetite 50:1–11. https://doi.org/10.1016/j.appet.2007.07.002

Marciniak E, Leboucher A, Caron E, Ahmed T, Tailleux A, Dumont J, Issad T, Gerhardt E, Pagesy P, Vileno M, Bournonville C, Hamdane M, Bantubungi K, Lancel S, Demeyer D, Eddarkaoui S, Vallez E, Vieau D, Humez S, Faivre E, Grenier-Boley B, Outeiro TF, Staels B, Amouyel P, Balschun D, Buee L, Blum D (2017) Tau deletion promotes brain insulin resistance. J Exp Med 214:2257–2269. https://doi.org/10.1084/jem.20161731

Mullins RJ, Diehl TC, Chia CW, Kapogiannis D (2017) Insulin resistance as a link between amyloid-beta and tau pathologies in Alzheimer's disease. Front Aging Neurosci 9:118. https://doi.org/10.3389/fnagi.2017.00118

Nunez J (2008) Morris water maze experiment. J Vis Exp. https://doi.org/10.3791/897

Papon MA, El Khoury NB, Marcouiller F, Julien C, Morin F, Bretteville A, Petry FR, Gaudreau S, Amrani A, Mathews PM, Hebert SS, Planel E (2013) Deregulation of protein phosphatase 2A and hyperphosphorylation of tau protein following onset of diabetes in NOD mice. Diabetes 62:609–617. https://doi.org/10.2337/db12-0187

Pennanen L, Wolfer DP, Nitsch RM, Gotz J (2006) Impaired spatial reference memory and increased exploratory behavior in P301L tau transgenic mice. Genes Brain Behav 5:369–379. https://doi.org/10.1111/j.1601-183X.2005.00165.x

Planel E, Tatebayashi Y, Miyasaka T, Liu L, Wang L, Herman M, Yu WH, Luchsinger JA, Wadzinski B, Duff KE, Takashima A (2007) Insulin dysfunction induces in vivo tau hyperphosphorylation through distinct mechanisms. J Neurosci 27:13635–13648. https://doi.org/10.1523/JNEUROSCI.3949-07.2007

Platt TL, Beckett TL, Kohler K, Niedowicz DM, Murphy MP (2016) Obesity, diabetes, and leptin resistance promote tau pathology in a mouse model of disease. Neuroscience 315:162–174. https://doi.org/10.1016/j.neuroscience.2015.12.011

Poulin SP, Dautoff R, Morris JC, Barrett LF, Dickerson BC, Alzheimer's Disease Neuroimaging I (2011) Amygdala atrophy is prominent in early Alzheimer's disease and relates to symptom severity. Psychiatry Res 194:7–13. https://doi.org/10.1016/j.pscychresns.2011.06.014

Reynolds CH, Garwood CJ, Wray S, Price C, Kellie S, Perera T, Zvelebil M, Yang A, Sheppard PW, Varndell IM, Hanger DP, Anderton BH (2008) Phosphorylation regulates tau interactions with Src homology 3 domains of phosphatidylinositol 3-kinase, phospholipase Cgamma1, Grb2, and Src family kinases. J Biol Chem 283:18177–18186. https://doi.org/10.1074/jbc.M709715200

Roozendaal B, Griffith QK, Buranday J, De Quervain DJ, McGaugh JL (2003) The hippocampus mediates glucocorticoid-induced impairment of spatial memory retrieval: dependence on the basolateral amygdala. Proc Natl Acad Sci USA 100:1328–1333. https://doi.org/10.1073/pnas.0337480100

Schubert M, Gautam D, Surjo D, Ueki K, Baudler S, Schubert D, Kondo T, Alber J, Galldiks N, Kustermann E, Arndt S, Jacobs AH, Krone W, Kahn CR, Bruning JC (2004) Role for neuronal insulin resistance in neurodegenerative diseases. Proc Natl Acad Sci USA 101:3100–3105. https://doi.org/10.1073/pnas.0308724101

Talbot K, Wang HY, Kazi H, Han LY, Bakshi KP, Stucky A, Fuino RL, Kawaguchi KR, Samoyedny AJ, Wilson RS, Arvanitakis Z, Schneider JA, Wolf BA, Bennett DA, Trojanowski JQ, Arnold SE (2012) Demonstrated brain insulin resistance in Alzheimer's disease patients is associated with IGF-1 resistance, IRS-1 dysregulation, and cognitive decline. J Clin Invest 122:1316–1338. https://doi.org/10.1172/JCI59903

Torres AK, Jara C, Olesen MA, Tapia-Rojas C (2021) Pathologically phosphorylated tau at S396/404 (PHF-1) is accumulated inside of hippocampal synaptic mitochondria of aged Wild-type mice. Sci Rep 11:4448. https://doi.org/10.1038/s41598-021-83910-w

Vorhees CV, Williams MT (2006) Morris water maze: procedures for assessing spatial and related forms of learning and memory. Nat Protoc. https://doi.org/10.1038/nprot.2006.116

Walf AA, Frye CA (2007) Estradiol decreases anxiety behavior and enhances inhibitory avoidance and gestational stress produces opposite effects. Stress 10:251–260. https://doi.org/10.1080/00958970701220416

Wijesekara N, Goncalves RA, Ahrens R, De Felice FG, Fraser PE (2018) Tau ablation in mice leads to pancreatic beta cell dysfunction and glucose intolerance. FASEB J 32:3166–3173. https://doi.org/10.1096/fj.201701352

Winzell MS, Ahren B (2004) The high-fat diet-fed mouse: a model for studying mechanisms and treatment of impaired glucose tolerance and type 2 diabetes. Diabetes 53(Suppl 3):S215–S219. https://doi.org/10.2337/diabetes.53.suppl_3.s215

Xia Y, Prokop S, Giasson BI (2021) "Don't Phos Over Tau": recent developments in clinical biomarkers and therapies targeting tau phosphorylation in Alzheimer's disease and other tauopathies. Mol Neurodegener 16:37. https://doi.org/10.1186/s13024-021-00460-5

Yang Y, Smith DL Jr, Keating KD, Allison DB, Nagy TR (2014) Variations in body weight, food intake and body composition after long-term high-fat diet feeding in C57BL/6J mice. Obesity (Silver Spring) 22:2147–2155. https://doi.org/10.1002/oby.20811

Authors and Affiliations

Jing Xiong[1,2] · Isaac Deng[1] · Sally Kelliny[1,3] · Liying Lin[1] · Larisa Bobrovskaya[1] · Xin-Fu Zhou[1]

✉ Jing Xiong
xiongjing@kmmu.edu.cn

✉ Xin-Fu Zhou
Xin-Fu.Zhou@unisa.edu.au

[1] School of Pharmacy and Medical Sciences, Division of Health Sciences, University of South Australia, Adelaide, SA, Australia

[2] Department of Neurology, the Second Affiliated Hospital, Kunming Medical University, Kunming, Yunnan Province, China

[3] Faculty of Phamacy, Assiut University, Assiut, Egypt